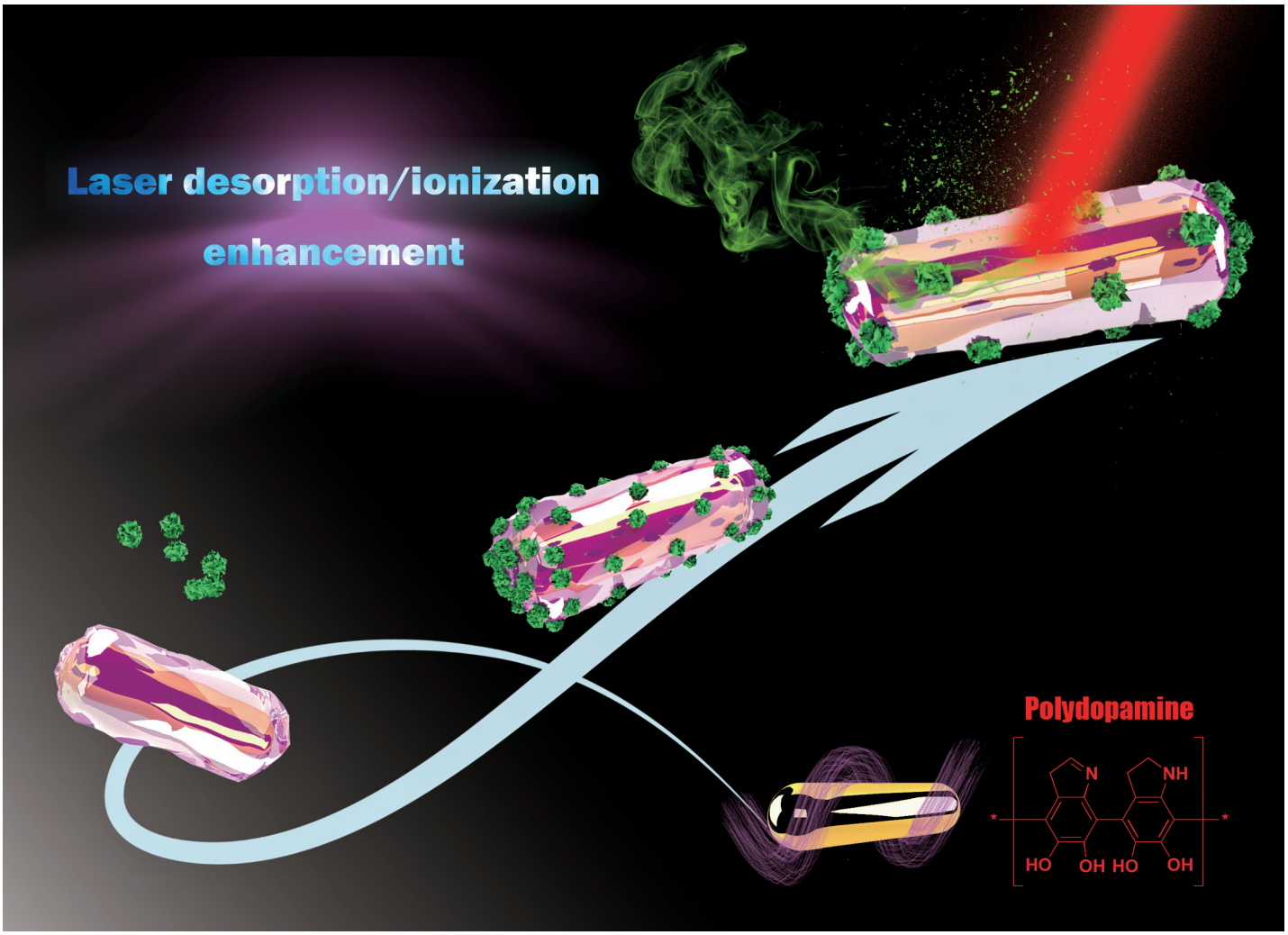

Showcasing research from the Dr Young-Kwan Kim at the Carbon Composite Research Center, Institute of Advanced Composite Materials, Korea Institute of Science and Technology, Jeonrabuk-do, Wanju-gun, Korea, and co-authors.

The influence of polydopamine coating on gold nanorods for laser desorption/ionization time-of-flight mass spectrometric analysis

The effect of polydopamine coating on gold nanorods for laser desorption/ionization time-of-light mass spectrometry (LDI-TOF-MS) analysis was investigated. We found that the polydopamine coating on the gold nanorods suppressed the generation of undesired gold cluster ions and enhanced the LDI-TOF-MS efficiency.

As featured in:

See Young-Kwan Kim *et al.*, *Analyst*, 2017, **142**, 2372.

ROYAL SOCIETY OF CHEMISTRY

rsc.li/analyst

Registered charity number: 207890

Analyst

PAPER

View Article Online
View Journal | View Issue

Cite this: *Analyst*, 2017, **142**, 2372

The influence of polydopamine coating on gold nanorods for laser desorption/ionization time-of-flight mass spectrometric analysis†

Kyungtae Kang,‡[a] Hongje Jang‡[b] and Young-Kwan Kim *[c]

Received 28th February 2017,
Accepted 9th May 2017

DOI: 10.1039/c7an00356k

rsc.li/analyst

This paper examines the effect of polydopamine (PD) coating of gold nanorods (GNRs) on their performance as a matrix material for laser desorption/ionization time-of-flight mass spectrometry (LDI-TOF-MS) analysis. Bare GNRs and PD-coated GNRs (PD@GNRs) were utilized for LDI-TOF-MS analyses of small molecules and synthetic polymers, and the influences of PD-coating were mechanistically studied. Based on the results, we found that the PD-coating of GNRs suppressed the generation of undesired gold cluster ions, enhanced photothermal conversion and the LDI-TOF-MS efficiency, and expanded the working molecular weight range.

Introduction

Matrix-assisted laser desorption/ionization time-of-flight mass spectrometry (MALDI-TOF-MS) is one of the most powerful analytical tools for peptides, proteins and synthetic polymers based on its capability of high-throughput analysis with high resolution and sensitivity.[1] However, this technique has not been directly applied to analyzing small molecules because of the matrix interference that occurs in the low-mass region (<500 Da).[2] Direct laser desorption/ionization time-of-flight mass spectrometry (LDI-TOF-MS) enables the analysis of organic materials but it also requires high laser power.[3] For addressing this issue, various nanomaterials including metals,[4,5] semiconductors[6,7] and carbon nanostructures[8–10] have been introduced as a mediator for soft LDI-TOF-MS analysis.

For the successful LDI-TOF-MS analysis of small molecules with these nanostructures, an appropriate surface coating layer is required to prevent the surface oxidation of the matrix material[11] and analyte fragmentation,[12] and to enhance the colloidal stability of the matrix material and LDI-TOF-MS efficiency.[13] To this end, various coating materials have been incorporated, such as self-assembled monolayers of organic molecules,[14,15] carbon,[16] SiO_2,[17] TiO_2,[18] and polydopamine (PD).[19–21] Among others, PD-coating has been recently investigated to develop multifunctional LDI-TOF-MS platforms that enable the enrichment of pollutants[19] or phosphorylated peptides.[20] In addition, the PD-coating could make the hydrophobic nanomaterials dispersible in water. The PD-coating on carbon nanotubes (CNTs) enhanced considerably their water dispersity and LDI-TOF-MS analysis efficiency for detecting various small molecules.[21] These results showed great promise of PD-coating for LDI-TOF-MS analysis, but the influence of PD-coating on LDI-TOF-MS has not been clearly understood, since the enrichment studies mentioned above also used an assistant organic matrix, and CNTs have high LDI-TOF-MS efficiency that overwhelms the contributions of other minor compounds to LDI-TOF-MS.[22]

Therefore, in order to exclusively investigate the effect of PD-coating on LDI-TOF-MS, an appropriate model that satisfies the following criteria is required: well-defined structures, high dispersity in solvents and low LDI-TOF-MS efficiency with a UV laser source. In this regard, gold nanorods (GNRs) are an interesting candidate, since GNRs exhibit high aqueous dispersity and a wavelength-dependent photothermal conversion property that originates from their two surface plasmon resonance (SPR) modes along the transversal and longitudinal directions.[23] The longitudinal direction has been utilized for the LDI-TOF-MS analysis of small peptides with a NIR laser source,[24] since it presents a higher SPR efficiency than the transversal direction. PD-coated gold nanomaterials have not been explored for LDI-TOF-MS analysis and it is thus important to clarify the effect of PD-coating on LDI-TOF-MS with GNRs, considering the widespread applications of gold nanomaterials in this field.[25–27]

[a]*Department of Applied Chemistry, Kyung Hee University, Yongin, Gyeonggi 446-701, South Korea*
[b]*Department of Chemistry, Kwangwoon University, 20, Gwangwoon-ro, Nowon-gu, Seoul 139-701, Korea*
[c]*Carbon Composite Materials Research Center, Institute of Advanced Composite Materials, Korea Institute of Science and Technology, San 101, Eunha-ri, Bongdong-eup, Wanju-gun, Jeollabuk-do, 565-905, Korea.*
E-mail: youngkwan@kist.re.kr

†Electronic supplementary information (ESI) available. See DOI: 10.1039/c7an00356k

‡Equally contributed to this manuscript.

Fig. 1 Scheme of the synthesis and LDI-TOF-MS application of GNR and PD@GNR.

Herein, we synthesized GNRs and PD@GNRs and characterized them by using transmission electron microscopy (TEM), UV-Vis, and Raman spectroscopies. The synthesized GNRs and PD@GNRs were applied to the LDI-TOF-MS analysis of a model thermometer molecule to reveal the processes of energy conversion that occur on their surfaces during the LDI-TOF-MS process (Fig. 1). Then, GNRs and PD@GNRs were applied to the LDI-TOF-MS analyses of small molecules and synthetic polymers. Based on the results, we found that PD layers on the surface of GNRs significantly suppress the formation of Au cluster ions, enhance photothermal conversion and the LDI-TOF-MS efficiency, and expand the working molecular weight range. This strategy will be useful for the mass spectrometric analysis of small molecules and synthetic polymers by using every type of laser desorption/ionization mass spectrometry (LDI-MS).

Experimental

Materials

Hydrogen tetrachloroaurate(III) hydrate was purchased from Kojima Chemicals (Japan). Cetyltrimethylammonium bromide (CTAB), silver nitrate, sodium borohydride, ascorbic acid, glucose, glucosamine, sucrose and polyethylene glycol (PEG) having different M_ws (500, 1000, 2000 and 4000) were purchased from Alfa Aesar (Ward Hill, USA). Tris(hydroxymethyl) aminomethane (Tris) was purchased from Deajung Chemicals (Siheung, Korea). All chemicals were used as received.

Synthesis of GNRs

GNRs were synthesized by a previously reported protocol.[28] In detail, a seed solution was prepared by addition of 250 μL of 10 mM solution of $HAuCl_4$ to 7.5 mL of 100 mM CTAB solution. The mixture was gently mixed by shaking. The color of the mixture was bright brown-yellow. Then, 600 μL of 10 mM ice-cooled $NaBH_4$ solution was added to the mixture at once and the mixture was gently shaken for 2 min. The prepared seed solution was kept for 6 h before use. A growing solution was prepared by addition of 2 mL of 10 mM $HAuCl_4$ and 300 μL of 10 mM $AgNO_3$ to 47.5 mL of 100 mM CTAB solution. The mixture was mixed by gentle shaking. 320 μL of 100 mM ascorbic acid solution was added to the mixture. Finally, 100 μL of the seed solution was added to the prepared growing solution and the mixture was gently shaken for 10 s and kept overnight without disturbance. GNRs in the reaction mixture were purified by centrifugation at 12 857 rcf and re-suspension into distilled water 2 times.

Synthesis of PD@GNRs

PD@GNRs were synthesized by a previously reported procedure.[29] The synthesized GNR suspension was centrifuged at 12 857 rcf and re-dispersed in 50 mL of 10 mM Tris buffer (pH 8.5) containing 6 mg of dopamine hydrochloride. The suspension was shaken for 4 h. The reaction mixture was centrifuged again at 12 857 rcf and washed with water three times.

Synthesis of benzylpyridinium salt (BP)

7.8 g of benzyl bromide (45.5 mmol) was added to 3.0 g of pyridine (37.9 mmol) in a 20 mL vial with stirring. The reaction was carried out at 50 °C for 12 h. Afterwards, the formed precipitate was washed with diethyl ether, filtered, and washed with a copious amount of diethyl ether (95% yield). The BP was dissolved in methanol at 1 mM for LDI-TOF-MS analysis.[30]

LDI-TOF-MS analysis

1 μL of each GNR and PD@GNR suspension was spotted on a stainless steel plate, dried under ambient conditions and subjected to LDI-TOF-MS analysis. For LDI-TOF-MS analysis of small molecules, 1 μL of 100 μM BP, glucose, glucosamine and sucrose solutions was spotted on the plate, mixed with 1 μL of GNR or PD@GNR suspension, dried under ambient conditions and subjected to LDI-TOF-MS analysis. For synthetic polymers, 1 μL of 1 mg mL^{-1} PEG (M_w 500, 1000, 2000 and 4000) solutions was spotted on the plate, mixed with 1 μL of GNR and PD@GNR suspensions, dried under ambient conditions and subjected to LDI-TOF-MS analysis. All LDI-TOF-MS analyses were carried out by using a Bruker Autoflex III (Bruker Daltonics, Germany) equipped with a Smartbeam laser (Nd:YAG, 355 nm, 100 Hz, 100 μJ of laser power, 30 μm of spot diameter at the target plate) in positive reflective mode at 38–80% laser power. The accelerating voltage was 19 kV and all spectra were obtained by averaging 500 laser shots irradiated in random work mode over a partial sample unless otherwise indicated.

Characterization

The size and shape of GNRs and PD@GNRs were observed by using a Tecnai G2 F30 Field Emission TEM (FEI Company, Netherlands). UV-Vis-NIR spectra were recorded with a J670 (Jasco, Japan) using a quartz substrate. Zeta potentials of GNR and PD@GNR were analysed by using a Nano ZS (Malvern, UK). Raman spectra of GNRs and PD@GNRs were obtained by using a Horiba LabRAM (Jobin Yvon, France) using an air-cooled He/Ne laser (514 nm) as an excitation source focused through an integral microscope (Olympus BX 41). A Raman scattering signal was detected with a 180° geometry using an air-cooled 1024 × 256 pixel CCD detector.

Results and discussion

GNRs were synthesized and coated with PD through the self-oxidative polymerization of dopamine in Tris buffer (pH 8.5). The width and length of the GNRs were around 10 nm and 50 nm, respectively (aspect ratio: 5) (Fig. 2a). After the reaction,

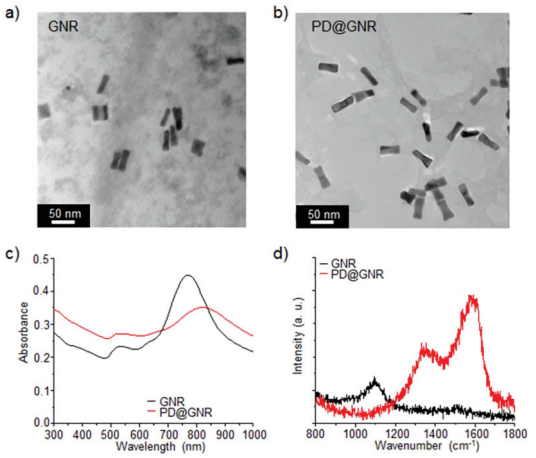

Fig. 2 TEM images (a, b), UV-Vis-NIR (c) and Raman (d) spectra of GNR and PD@GNR.

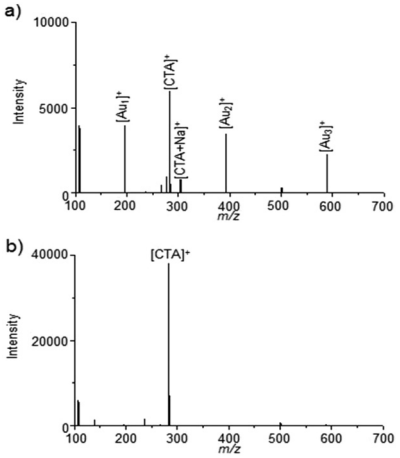

Fig. 3 LDI-TOF-MS spectra of GNR (a) and PD@GNR (b). The applied laser energy was 50 μJ.

the GNRs were coated with a thin layer of amorphous carbon with slight aggregation (Fig. 2b). To further confirm the formation of the PD layer on GNRs, the change of surface charge was examined by zeta potential analysis. The zeta potential of GNRs was highly positive (58.8 mV) because of the CTAB bilayer on their surfaces[31] but this value turned negative (−24.3 eV) after the PD-coating, presumably because of abundant phenol groups.[32] The UV-Vis-NIR spectra of GNRs exhibited typical two SPR modes, the transversal mode at 530 nm and the longitudinal mode at 770 nm. PD@GNRs also showed two SPR modes but their positions were red-shifted to 535 nm and 820 nm, respectively, compared to those with pristine GNRs. These changes originate from the changes in the reflective index around the surface of the GNRs (Fig. 2c).[33] The typical D- and G-bands of the PD layer were observed from the Raman spectra of PD@GNRs (Fig. 2d).[34] The characterization results clearly proved that the PD@GNRs were successfully synthesized by our synthetic methods.

GNRs and PD@GNRs were then subjected to LDI-TOF-MS analysis with 50 μJ laser energy. The LDI-TOF-MS spectra of GNRs presented strong gold cluster ion peaks at m/z 196 $[Au_1]^+$, 393 $[Au_2]^+$ and 590 $[Au_3]^+$, and the cetyltrimethylammonium (CTA) ion peak at m/z 283 (Fig. 3a).[35] The detection of CTA ions is attributed to the direct laser desorption/ionization (LDI) of the CTAB bilayer on GNR surfaces. By contrast, PD@GNR only showed CTA ions under the same LDI-TOF-MS analysis conditions and this result implied that the PD-coating layer prevented the direct detection of gold cluster ions (Fig. 3b). An analogous trend was also observed with low laser energy (38 μJ) indicating that the signal enhancement and suppression of Au-related ion signals were due to the PD-coating layer rather than the high laser energy (Fig. S1 in the ESI†). Since the generation of gold cluster ions leads to formation of undesired adducts and makes the interpretation of the mass spectrum complex, this result indicates that PD-coating on gold nanostructures greatly improves their performance in LDI-TOF-MS analysis.

The standard thermometer molecule, BP, was analysed with LDI-TOF-MS under 42 μJ laser irradiation by using GNRs and PD@GNRs to examine the detailed LDI-TOF-MS process on their surfaces (Fig. 4). The desorption efficiency (DE) and

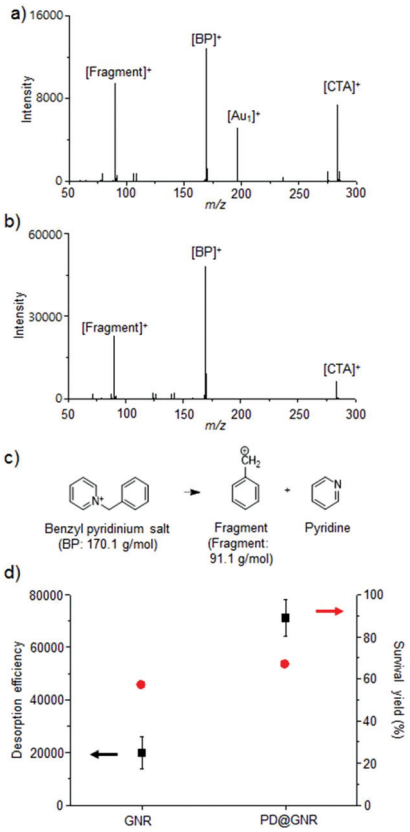

Fig. 4 LDI-TOF-MS spectra of BP obtained with GNR (a) and PD@GNR (b). (c) Fragmentation reaction of BP during the LDI-TOF-MS analysis process. (d) Average DE and SY of BP with GNR and PD@GNR. The average DE and SY values were obtained from 5 measurements in the different regions of each spot. The applied laser energy was 42 μJ.

survival yield (SY) of BP were respectively estimated by summing the intensities of the parent and fragmented BP ions, and dividing the parent ion with the fragmented ion intensity (Fig. 4a–c).[36] The average DE value of BP with GNRs was 19 882 ± 6196 and the relatively low value can be attributed to the low UV laser energy absorption capacity and energy transfer efficiency by unintended laser energy decay through LDI of gold cluster ions. The DE value increased to 71 175 ± 6853 with PD@GNRs (Fig. 4d). This drastic increase of DE implied that the PD-coating of GNRs not only suppressed LDI of gold cluster ions but also enhanced LDI of BP by improving the photothermal conversion efficiency. The average SY value of GNRs was 57 ± 2.0% and this value also increased to 67 ± 0.7% for PD@GNRs (Fig. 4d). These results partially suggest that PD-coating of GNRs greatly improves their performance as a mediator for LDI-TOF-MS analysis. The energy-dependent LDI-TOF-MS analysis of BP with GNRs and PD@GNRs further confirmed that BP was softly desorbed and ionized by PD@GNRs with a high mass signal compared to GNRs (Fig. S2†). Still, different surface charges of GNRs and PD@GNRs may have caused the observed different photothermal properties: BP is positively charged and thus will interact more strongly with negatively charged PD@GNRs than positively charged GNRs. Thus, to exclude this possibility, analyses of various small molecules should be compared between experimental conditions that use GNRs and PD@GNRs.

Amino acids and saccharides were selected among other small molecules because they are important metabolites and thus are frequent target analytes in LDI-TOF-MS analysis.[37] Arginine, phenylalanine, glucose, glucosamine, sucrose and cellobiose (100 pmol) were analysed with GNRs and PD@GNRs. When using GNR as a matrix, only gold cluster and CTA ions were detected without the corresponding mass peaks of the analytes (Fig. 5). On the other hand, all these small molecules were successfully detected at *m*/*z* 202 [glucose + Na]$^+$, 201 [glucosamine + Na]$^+$, 364 [sucrose + Na]$^+$, 175 [arginine + H]$^+$ and 196 [arginine + Na]$^+$, 188 [phenylalanine + Na]$^+$ and 210 [phenylalanine + 2Na]$^+$ and 364 [cellobiose + Na]$^+$ by using PD@GNRs without gold cluster ions (Fig. 5). The unassigned mass peaks in mass spectra might originate from the thermal fragmentation of the CTAB layer and PD-coating layer during the LDI-TOF-MS analysis.[38,39] Their detectable concentrations were measured to be 1 nmol for arginine and phenylalanine, 100 pmol for glucose, cellobiose and sucrose, and 10 pmol for glucosamine (Fig. S3†). No mass signal was detected from the spots of pure small molecules on blank targets without GNRs and PD@GNRs (Fig. S4†). This result indicated that the LDI-TOF-MS signals were obtained by the matrix assisted effect from the PD-coating. For further confirming this effect, LDI-TOF-MS analysis of small molecules was conducted on a PD coated steel substrate and all of the analytes were detected on the substrate (Fig. S5†). This result was in accordance with the results from the LDI-TOF-MS analysis of BP and thus confirmed that the PD-coating layer suppresses the LDI of gold cluster ions and enhances the LDI-TOF-MS analysis efficiency. For examination of the distribution effect of analyses/

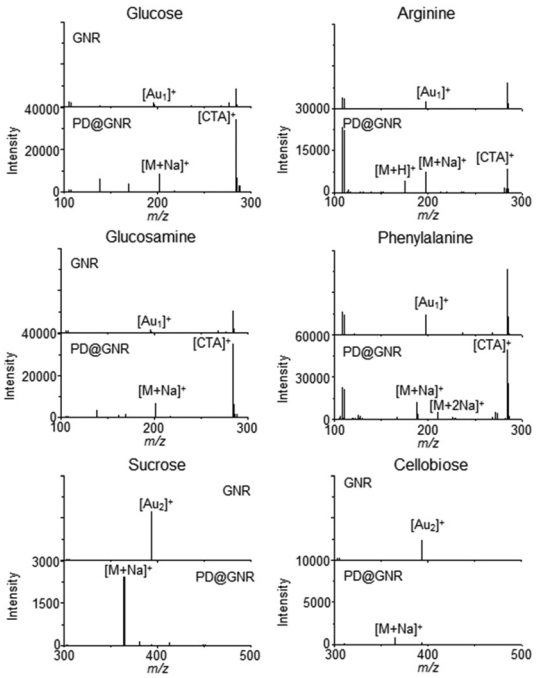

Fig. 5 LDI-TOF-MS spectra of 1 nmol glucose, glucosamine, sucrose, arginine, phenylalanine and cellobiose obtained by using GNR and PD@GNR with 42 μJ laser energy.

PD@GNRs on their LDI-TOF-MS behaviour, cellobiose was analysed in different regions of its spot mixed with PD@GNR. The mass signal was stronger along the edge of the spot than the central region owing to the coffee ring effect although the mass signal was detected at any points (Fig S6,† and see Fig. S7 and S8† for the LDI-TOF-MS analysis of BP with GNR and PD@GNR).[40,41]

The influence of PD-coating on the working molecular weight of LDI-TOF-MS analysis was explored by using PEGs with different M_ws. PEGs (1 μg) having different M_ws (500, 1000, 2000 and 4000 Da) were analysed using GNR and PD@GNR. PEG_{500} and PEG_{1000} could be detected without any matrix, and showed peaks with an interval of 28 and 44 Da corresponding to their fragmented species (–CH_2–CH_2–) and repeating unit of PEG (–CH_2–CH_2–O–).[42] However, PEG_{2000} and PEG_{4000} were not detected even with support of GNR (Fig. 6). Although GNR did not extend the working molecular weight range, it is noteworthy that GNR enhanced the ion intensities of PEG_{1000} and its degree of fragmentation because this enhancement implied that GNR could itself improve the LDI-TOF-MS analysis efficiency through the thermal desorption process (Fig. 6). By contrast, all PEGs were successfully detected by using PD@GNR with the reduced degree of fragmentation compared to direct and the results obtained with GNR (Fig. 6). This result proved that the PD-coating expanded the working molecular weight range of LDI-TOF-MS analysis using GNR as a matrix material. The figures of merit (FOM) such as M_n, M_w, polydispersity index (PDI), signal to noise ratio (S/N) and resolution from the LDI-TOF-MS analysis of

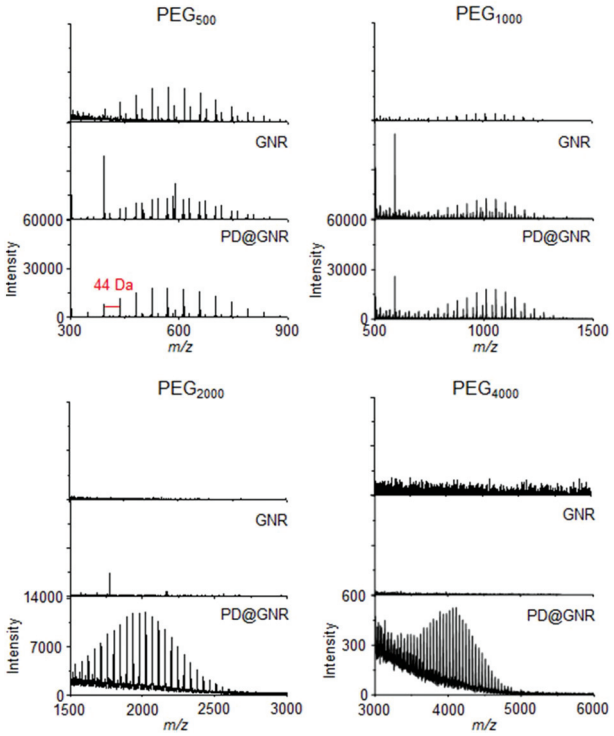

Fig. 6 LDI-TOF-MS spectra of PEGs with different M_ws 500, 1000, 2000 and 4000 Da and their LDI-TOF-MS spectra obtained with GNR and PD@GNR. The applied laser energy was 80 μJ.

PEG derivatives are summarized in Fig. S9.† The obtained M_n, M_w and PDI values were only slightly deviated from the values obtained by gel permeation chromatography (GPC) provided in the supplier information. The deviation might stem from the methodological difference. Importantly, the S/N values increased in the order of PEG themselves, PEG with GNR and PEG with PD@GNR. To further examine the influence of the PD-coating layer on the LDI-TOF-MS analysis of synthetic polymers, the polyethylene-*block*-PEG_{1500} (PE-*b*-PEG) and PEG-*block*-polypropylene glycol-*block*-PEG_{5800} (PEG-*b*-PPG-*b*-PEG) were analysed with GNR and PD@GNR. In concurrence with the LDI-TOF-MS analysis of PEG derivatives, PE-*b*-PEG and PEG-*b*-PPG-*b*-PEG were only detected with PD@GNR (Fig. S10†). These results further confirmed that the PD-coating enhances the LDI-TOF-MS analysis of PEG derivatives.

Conclusions

In conclusion, the influences of the PD-coating layer on the LDI-TOF-MS analysis of small molecules and synthetic polymers were systematically investigated by using GNRs as a model support nanomaterial. The generation of PD@GNRs (PD-coating of GNRs) caused the considerably suppressed generation of gold cluster ions, enhanced the LDI efficiency, and expanded the working molecular weight range during LDI-TOF-MS analysis. The improved performance of PD@GNR compared to GNR was attributed clearly to the versatility of PD layers, which prevented direct gold cluster ionization, and largely enhanced the laser energy absorption capacity and photothermal conversion efficiency. These results successfully demonstrated the important advantages of PD-coating of the gold nanostructures for LDI-TOF-MS analysis. The most important potential of our strategy is the wide applicability to other efficient LDI-TOF-MS platforms such as carbon, metal and semiconductor nanoparticles and/or porous films based on the universal adhesion property of the PD layer.[38] This wide applicability is also beneficial for LDI-TOF-MS based imaging[43] and combination with MALDI-TOF-MS imaging analysis of metabolites, lipids, and small peptides.[41,44] We believe that this study provides useful insights and background to develop a highly efficient analytical platform with not only LDI-TOF-MS but also every type of LDI-MS.

Acknowledgements

This research was financially supported by grants from the Korea Institute of Science and Technology (KIST) institutional program and the Nano Material Technology Development Program through the National Research Foundation of Korea (NRF) funded by the Ministry of Science, ICT and Future Planning (2016 M3A7B4027223 and 2016 M3A7B4905609). This work was also supported by a grant from Kyung Hee University in 2016 (KHU-20160610).

Notes and references

1 M. Karas and F. Hillenkamp, *Anal. Chem.*, 1988, **60**, 2299.
2 D. S. Peterson, *Mass Spectrom. Rev.*, 2007, **26**, 19.
3 F. Hillenkamp, E. Unsöld, R. Kaufmann and R. Nitsche, *Nature*, 1975, **256**, 119.
4 J. A. McLean, K. A. Stumpo and D. H. Russell, *J. Am. Chem. Soc.*, 2005, **127**, 5304.
5 J. Sekuła, J. Nizioł, W. Rode and T. Ruman, *Analyst*, 2015, **140**, 6195.
6 M. Yang and T. Fujino, *Anal. Chem.*, 2014, **86**, 9563.
7 H. Sato, A. Nemoto, A. Yamamoto and H. Tao, *Rapid Commun. Mass Spectrom.*, 2009, **23**, 603.
8 J. Wang, Q. Liu, Y. Liang and G. Jiang, *Anal. Bioanal. Chem.*, 2016, **408**, 2861.
9 Y.-K. Kim and D.-H. Min, *Chem. – Eur. J.*, 2015, **21**, 7217.
10 Y.-K. Kim and D.-H. Min, *Langmuir*, 2014, **30**, 12675.
11 S. Vaidyanathan, D. Jones, J. Ellis, T. Jenkins, C. Chong, M. Anderson and R. Goodacre, *Rapid Commun. Mass Spectrom.*, 2007, **21**, 2157.
12 M. E. Kurczy, Z. J. Zhu, J. Ivanisevic, A. M. Schuyler, K. Lalwani, A. F. Santidrian, J. M. David, A. Giddabasappa, A. J. Roberts, H. J. Olivos, P. J. O'Brien, L. Franco, M. W. Fields, L. P. Paris, M. Friedlander, C. H. Johnson, A. A. Epstein, H. E. Gendelman, M. R. Wood, B. H. Felding,

G. J. Patti, M. E. Spilker and G. Siuzdak, *Nat. Commun.*, 2015, **6**, 5998.
13 I. Alessandri, I. Vassalini, M. Bertuzzi, N. Bontempi, M. Memo and A. Gianoncelli, *Sci. Rep.*, 2016, **6**, 34521.
14 A. L. Marsico, G. S. Elci, D. F. Moyano, G. Yesilbag Tonga, B. Duncan, R. F. Landis, V. M. Rotello and R. W. Vachet, *Anal. Chem.*, 2015, **87**, 12145.
15 G. Luo, Y. Chen, G. Siuzdak and A. Vertes, *J. Phys. Chem. B*, 2005, **109**, 24450.
16 G. Xu, S. Liu, J. Peng, W. Lv and R. Wu, *ACS Appl. Mater. Interfaces*, 2015, **7**, 2032.
17 X. Zhu, L. Wu, D. C. Mungra, S. Xia and J. Zhu, *Analyst*, 2012, **137**, 2454.
18 C. T. Chen and Y. C. Chen, *Anal. Chem.*, 2005, **77**, 5912.
19 Y. R. Ma, X. L. Zhang, T. Zeng, D. Cao, Z. Zhou, W. H. Li, H. Niu and Y. Q. Cai, *ACS Appl. Mater. Interfaces*, 2013, **5**, 1024.
20 M. Zhao, C. Deng and X. Zhang, *ACS Appl. Mater. Interfaces*, 2013, **5**, 13104.
21 C. Shi, C. Deng, X. Zhang and P. Yang, *ACS Appl. Mater. Interfaces*, 2013, **5**, 7770.
22 Y.-K. Kim and D.-H. Min, *ACS Appl. Mater. Interfaces*, 2012, **4**, 2088.
23 A. M. Alkilany, L. B. Thompson, S. P. Boulos, P. N. Sisco and C. J. Murphy, *Adv. Drug Delivery Rev.*, 2012, **64**, 190.
24 E. T. Castellana, R. C. Gamez, M. E. Gómez and D. H. Russell, *Langmuir*, 2010, **26**, 6066.
25 B. Yan, S. T. Kim, C. S. Kim, K. Saha, D. F. Moyano, Y. Xing, Y. Jiang, A. L. Roberts, F. S. Alfonso, V. M. Rotello and R. W. Vachet, *J. Am. Chem. Soc.*, 2013, **135**, 12564.
26 H. Seo, S. Kim, J. I. Kim, H. Kang, W. Jung and W. S. Yeo, *Anal. Biochem.*, 2013, **434**, 199.
27 H. Z. Lai, S. G. Wang, C. Y. Wu and Y. C. Chen, *Anal. Chem.*, 2015, **87**, 2114.
28 J. G. Hinman, A. J. Stork, J. A. Varnell, A. A. Gewirth and C. J. Murphy, *Faraday Discuss.*, 2016, **191**, 9.
29 K. C. Black, T. S. Sileika, J. Yi, R. Zhang, J. G. Rivera and P. B. Messersmith, *Small*, 2014, **10**, 169.
30 Y.-K. Kim and D.-H. Min, *Langmuir*, 2012, **28**, 4453.
31 S. Gómez-Graña, F. Hubert, F. Testard, A. Guerrero-Martínez, I. Grillo, L. M. Liz-Marzán and O. Spalla, *Langmuir*, 2012, **28**, 1453.
32 A. Ma, Y. Xie, J. Xu, H. Zeng and H. Xu, *Chem. Commun.*, 2015, **51**, 1469.
33 H. Zhang, D. Song, S. Gao, H. Zhang, J. Zhang and Y. Sun, *Talanta*, 2013, **115**, 857.
34 J. Ryu, S. H. Ku, H. Lee and C. B. Park, *Adv. Funct. Mater.*, 2010, **20**, 2132.
35 I. García, M. Henriksen-Lacey, A. Sánchez-Iglesias, M. Grzelczak, S. Penadés and L. M. Liz-Marzán, *J. Phys. Chem. Lett.*, 2015, **6**, 2003.
36 Y.-K. Kim, H.-K. Na, S.-J. Kwack, S.-R. Ryoo, Y. Lee, S. Hong, S. Hong, Y. Jeong and D.-H. Min, *ACS Nano*, 2011, **5**, 4550.
37 C. W. Tsao and Z. J. Yang, *ACS Appl. Mater. Interfaces*, 2015, **7**, 22630.
38 H. Lee, S. M. Dellatore, W. M. Miller and P. B. Messersmith, *Science*, 2007, **318**, 426.
39 Y. Ding, L. T. Weng, M. Yang, Z. Yang, X. Lu, N. Huang and Y. Leng, *Langmuir*, 2014, **30**, 12258.
40 J. B. Hu, Y. C. Chen and P. L. Urban, *Anal. Chim. Acta*, 2013, **766**, 77.
41 A. L. Marsico, B. Duncan, R. F. Landis, G. Y. Tonga, V. M. Rotello and R. W. Vachet, *Anal. Chem.*, 2017, **89**, 3009.
42 T. Watanabe, H. Kawasaki, T. Yonezawa and R. Arakawa, *J. Mass Spectrom.*, 2008, **43**, 1063.
43 Q. Wu, J. L. Chu, S. S. Rubakhin, M. U. Gillette and J. V. Sweedler, *Chem. Sci.*, 2017, **8**, 3926.
44 M. Kompauer, S. Heiles and B. Spengler, *Nat. Methods*, 2017, **14**, 90.